Fake Geometric Brownian Motion And Its Option Pricing

Xingjian Xu

St Peter's College
University of Oxford



Dissertation for MSc in Mathematical and Computational Finance
Trinity Term 2011

Acknowledgement

First of all, I would like to express my heartfelt gratitude to my thesis supervisor, Dr Jan Obłój, for his support and encouragement. I am indebted for his valuable suggestions and advices when I encountered difficulties. I am grateful that I can learn not only the mathematical knowledge, but also the analytic way of thinking from him.

Secondly, I would like to acknowledge the efforts of all the department members who have taught and advised me during the MSc course, from which I deepened my understanding and made progress on both the theoretical and the numerical aspects for mathematical finance. I would also show my appreciations to my classmates and my friends, especially, Qing Liu, Cheng Zhu, and Yizun Gu, during the discussions with whom I obtained a lot of inspirations for treating the details.

Last but not least, I would like to devote my deepest gratitude to my parents. Any of my progress or achievement today could not be made without their continuous love and support to me.

Abstract

In this thesis, we begin with introducing the notion of a fake geometric Brownian motion in analogy to the fake Brownian motion. Secondly we construct two discontinuous fake geometric Brownian motion processes via the solutions to the Skorokhod embedding problem. Finally we simulate European and path-dependent option pricings for stock prices following these processes, to see how different the results can be compared with the traditional Black & Scholes setting.

Key words: *fake Brownian motion*, *fake geometric Brownian motion*, *Skorokhod embedding problem*, *Azéma-Yor solution*, *reversed Azéma-Yor solution*.

Contents

Introduction **1**

Recall of the classical Black & Scholes setting 2

1 "Fake" processes **4**

1.1 Definition of fake Brownian motions and fake geometric Brownian motions 4

1.2 Existence of fake Brownian motions - Construction of Oleszkiewicz . . 6

2 Skorokhod embedding **10**

2.1 Azéma-Yor embedding solution 10

2.1.1 Theory 10

2.1.2 Application on the marginals of GBM 13

2.2 Reversed Azéma-Yor embedding solution 19

2.2.1 Theory 19

2.2.2 Application on the marginals of GBM 20

3 Numerical considerations **22**

3.1 Stock prices at maturity 22

3.1.1 Generation of S_T without using Brownian bridge 22

3.1.2 Generation of S_T using Brownian bridge 25

3.2 Stock price paths 27

4 Option pricing **29**

4.1 European call option 29

4.2 One-touch option 31

4.3 Asian option 33

4.4 Variance swap 35

5 Conclusion and Final Remarks **36**

A Code Resources **37**

Introduction

In 1900, Bachelier demonstrated in his thesis [3] the necessity of choosing appropriate mathematical tools to price derivatives for the financial industry. He invented the mathematical notion of Brownian motion, and modelled the stock prices as a drifted Brownian motion. Such a modelling could lead to a negative stock price. Therefore, Samuelson ([13], 1965) proposed that instead of considering the stock price as a Brownian motion, it would be better to take into account the log return of the stock price. In addition, people found indeed that in reality, the log return of the stock price follows the normal distribution in general, except the fat tail for extremely rare events.

Considering the stock price as geometric Brownian motion was one of the most important assumptions in Black-Scholes-Merton option-pricing model ([4]) in 1973. From then on, the model of Black & Scholes became one of the core theories in the world of financial mathematics, and there has been an wide application for Black & Scholes formula, and its setting, not only for the original European option pricing, but also for the other exotic options, including the path-dependent ones.

From another aspect, a number of recent researches have been interested in studying and constructing martingales with given marginals. Albin ([1], 2008) has shown that there exists some continuous martingale processes different from the classical Brownian motion but having the same marginal distributions. Such processes are called *fake* Brownian motions.

It appears that somehow people don't always distinguish with intention the terminology of *geometric Brownian motion* processes and the terminology of *log-normal* distributions for describing the stock prices. With the two points of view listed above, our motivation of this thesis is to see whether there exists some martingale processes, or even continuous martingales processes, which is not a geometric Brownian motion,

but has the same marginal distributions, i.e. which follows the log-normal distribution at every time t. It is interesting to ask: how to construct such fake processes? Will there be some differences and what will be the differences if we do our option pricing with underlying asset following such processes? What is delicate behind the assumption of geometric Brownian motion in Black & Scholes setting? Is it possible to find any good construction following which the stock prices could be modelled to approximate the reality better?

We will answer some of the questions in this thesis. The outline of the thesis is as follows. In Chapter 1, we will introduce the definitions of fake Brownian motion and fake geometric Brownian motion, and show why the construction of the former cannot result in a direct construction of the latter. Then in Chapter 2, we study Skorokhod embedding problem and its solutions, and examine how they are applicable on our aimed marginal densities to construct two discontinuous fake geometric Brownian motions. Having obtained the theoretical part of the constructions, we carry out our numerical investigations in the following. Chapter 3 presents the numerical considerations for implementing the two fake processes, and Chapter 4 shows some numerical results for both European and path-dependent option pricings using the constructed fake processes as stock price, compared with the option prices under traditional Black & Scholes setting.

In the thesis, all the simulations and the graph presentations are realized by Matlab. A version of pseudo-code for the core parts of the code will be presented in Chapter 3.

For numerical applications, we use the initial stock price $S_0 = 100$, the maturity $T = 1$ (year), the interest rate $r = 0.02$, the volatility $\sigma = 0.3$ throughout the thesis.

Recall of the classical Black & Scholes setting

In the original article of Black and Scholes ([4], 1973), the European options are priced under the following assumptions:

- The short-term interest rate is known and constant through time;
- The stock price follows a geometric Brownian motion with constant volatility;
- The stock pays no dividends;

- There are no transaction costs;
- One can buy and sell any fraction of shares of the stock;
- Short-selling is permitted with no penalty.

In the following chapters of our thesis, we will note a such stock $S_t^{B\&S}$.

Moreover, for our fake geometric Brownian motions, we will also assume that in the marginal densities the interest rate and the volatility are constant. Hence, all of these assumptions hold as usual except some change for the second one.

Chapter 1

"Fake" processes

In order to compare with the new notion of fake processes, we recall the standard definition of Brownian motion and Lévy's characterization at the first place ([7, 12]).

Definition 1.0.1 (Brownian motion)**.** *On a probability space $(\Omega, \mathcal{F}, P)$, a real-valued stochastic process $(B_t)_{t\geqslant 0}$ is called a Brownian motion, if*

1. *$(B_t)_{t\geqslant 0}$ has independent increments with distribution $B_t - B_s \sim \mathcal{N}(0, t-s)$ for all $t > s \geqslant 0$;*
2. *B_t is continuous.*

The Brownian motion is called standard if it starts at 0, i.e. $P(B_0 = 0) = 1$.

Equivalently, we can define a Brownian motion as a continuous centred Gaussian process with covariance function $\mathrm{Cov}(B_t, B_s) = \min(s,t) := s \wedge t$.

Lévy's characterization is often considered as another way to define and identify Brownian motions.

Theorem 1.0.1 (Lévy's characterization)**.** *Let $(\Omega, \mathcal{F}, \mathcal{F}_t, P)$ be a filtered probability space. Let $(M_t)_{t\geqslant 0}$ be an adapted continuous local martingale with respect to $(\Omega, \mathcal{F}, \mathcal{F}_t, P)$. M is a Brownian motion if and only if the quadratic variation of M is equal to t, i.e. $\langle M, M\rangle_t = t$.*

1.1 Definition of fake Brownian motions and fake geometric Brownian motions

Consider a real-valued process $(X_t)_{t\geqslant 0}$ and let $(\mathcal{F}_t)_{t\geqslant 0}$ be the natural filtration associated with this process. We introduce here the notion of fake Brownian motion ([1, 11]).

Definition 1.1.1 (fake Brownian motion)**.** *The process $(X_t)_{t\geqslant 0}$ is a fake Brownian motion if it satisfies the following four conditions:*

1. *$(X_t)_{t\geqslant 0}$ has the same marginal densities as a classical Brownian motion $(B_t)_{t\geqslant 0}$: X_t follows the normal distribution with mean 0 and variance t for every $t \geqslant 0$, i.e.*
$$\forall t \geqslant 0, X_t \sim \mathcal{N}(0,t);$$
2. *X_t is continuous;*
3. *$(X_t)_{t\geqslant 0}$ is a martingale with respect to $(\mathcal{F}_t)_{t\geqslant 0}$;*
4. *$(X_t)_{t\geqslant 0}$ is not a genuine Brownian motion, i.e. it does not have the same joint distribution as $(B_t)_{t\geqslant 0}$.*

As from the first and the third conditions, we can derive that the process $(X_t)_{t\geqslant 0}$ has the same covariance structure as $(B_t)_{\geqslant 0}$ does,

$$\begin{aligned}\mathbb{E}(X_tX_s) &= \mathbb{E}(\mathbb{E}(X_tX_s|\mathcal{F}_s)) \\ &= \mathbb{E}(X_s\mathbb{E}(X_t|\mathcal{F}_s)) \\ &= \mathbb{E}(X_s^2) = s, \text{ for } t > s,\end{aligned}$$

the last condition is equivalent to require that $(X_t)_{t\geqslant 0}$ is not a Gaussian process. We will see the existence of such a process in the next section.

Similarly, we can give an analogous definition of fake geometric Brownian motions.

Definition 1.1.2 (fake geometric Brownian motion)**.** *The process $(X_t)_{t\geqslant 0}$ is a fake geometric Brownian motion (fake GBM) if it satisfies the following four conditions:*

1. *: $(X_t)_{t\geqslant 0}$ has the same marginal densities as a classical geometric Brownian motion: for every $t \geqslant 0$, X_t follows a log-normal distribution,*
$$\forall t \geqslant 0, X_t = \exp(\sigma Z_t + (r - \frac{\sigma^2}{2})t) \text{ where } Z_t \sim \mathcal{N}(0,t);$$
2. *X_t is continuous;*
3. *$(e^{-rt}X_t)_{t\geqslant 0}$ is a martingale with respect to $(\mathcal{F}_t)_{t\geqslant 0}$;*
4. *$(X_t)_{t\geqslant 0}$ does not have the same joint distribution as the classical geometric Brownian motion.*

1.2 Existence of fake Brownian motions - Construction of Oleszkiewicz

Hamza and Klebaner ([6]) proved in 2007 that there exists a large family of non-Gaussian processes which are martingales and have the same marginal distributions as a Brownian motion $(B_t)_{t\geqslant 0}$ does. Soon Albin ([1], 2008) gave a continuous construction of this, which confirmed the existence of fake Brownian motions. Here, we introduce the construction of Oleszkiewicz ([11]) which is not the first construction of fake Brownian motion, but a simpler one.

Let $(B_t)_{t\geqslant 0}$ and $(W_t)_{t\geqslant 0}$ be two standard Brownian motions. Let G_1 and G_2 be two random variables following the unit normal distribution $\mathcal{N}(0,1)$. $(B_t)_{t\geqslant 0}$, $(W_t)_{t\geqslant 0}$, G_1 and G_2 are independent. For a given $a \geqslant 0$, we define a filtration $\mathcal{F}_t^{(a)} := \sigma(G_1, G_2, (W_s)_{0\leqslant s\leqslant a+\ln t})$ for $t \geqslant e^{-a}$. Consider for $t \geqslant e^{-a}$,

$$X_t^{(a)} := \sqrt{t}(G_1 \cos W_{a+\ln t} + G_2 \sin W_{a+\ln t}).$$

$X_t^{(a)}$ is evidently continuous for $t \geqslant e^{-a}$. $(X_t^{(a)}, \mathcal{F}_t^{(a)})_{t\geqslant e^{-a}}$ is a martingale since

- $\forall t \geqslant e^{-a}$, $X_t^{(a)}$ is $\mathcal{F}_t^{(a)}$-measurable;
- $(X_t^{(a)})^2 \leqslant t(|G_1| + |G_2|)^2$ which is integrable, so $X_t^{(a)}$ is square integrable;
- Consider $Y_t = X_{e^{t-a}} = e^{\frac{t-a}{2}}(G_1 \cos W_t + G_2 \sin W_t)$, then

$$\begin{aligned} \mathrm{d}Y_t &= \frac{1}{2}Y_t \mathrm{d}t + e^{\frac{t-a}{2}} G_1(-\sin W_t \mathrm{d}W_t - \frac{1}{2}\cos W_t \mathrm{d}\langle W\rangle_t) \\ &\quad + e^{\frac{t-a}{2}} G_2(\cos W_t \mathrm{d}W_t - \frac{1}{2}\sin W_t \mathrm{d}\langle W\rangle_t) \\ &= e^{\frac{t-a}{2}}(-G_1 \sin W_t + G_2 \cos W_t)\mathrm{d}W_t, \end{aligned}$$

  which has no drift term. Since the map $t \mapsto e^{t-a}$ is strictly increasing, the martingale property is conserved with the time-change.

It is easy to see that for each $t \geqslant e^{-a}$, $X_t^{(a)} \sim B_t$, as

$$\begin{cases} G_1 \cos W_t + G_2 \sin W_t \\ -G_1 \sin W_t + G_2 \cos W_t \end{cases}$$

can be considered as a random rotation of the jointly independent normal distribution (G_1, G_2), and thus follows $\mathcal{N}(0, I_2)$ as well.

Note that for each path, $\lim_{t\to\infty}(sup_{0\leqslant s\leqslant t}|X_s^{(a)}|/\sqrt{s}) \leqslant |G_1| + |G_2| < \infty$ a.s., while $\lim_{t\to\infty}(sup_{0\leqslant s\leqslant t}|B_s|/\sqrt{s}) = \infty$ a.s. $(X_t^{(a)})_{t\geqslant e^{-a}}$ doesn't admit the property as a genuine Brownian motion does. (See Figure 1.3.)

By using Kolmogorov consistency theorem, this construction can be extended for $t \geqslant 0$ with associated newly-defined filtration. An interested reader may refer to the details in Oleszkiewicz's original work [11].

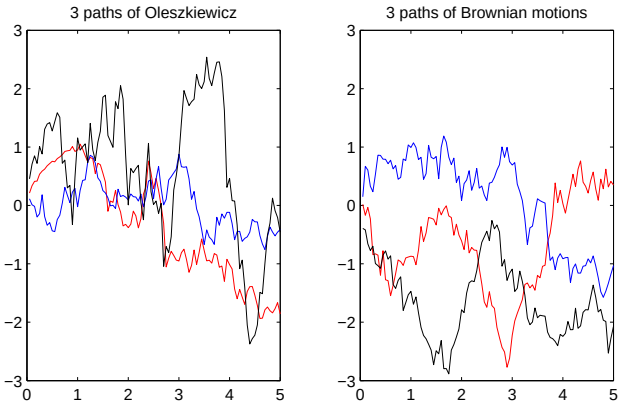

Figure 1.1: Comparison of 3 Oleszkiewicz paths and 3 Brownian motion paths: We see that Oleszkiewicz paths look the same as Brownian motion paths.

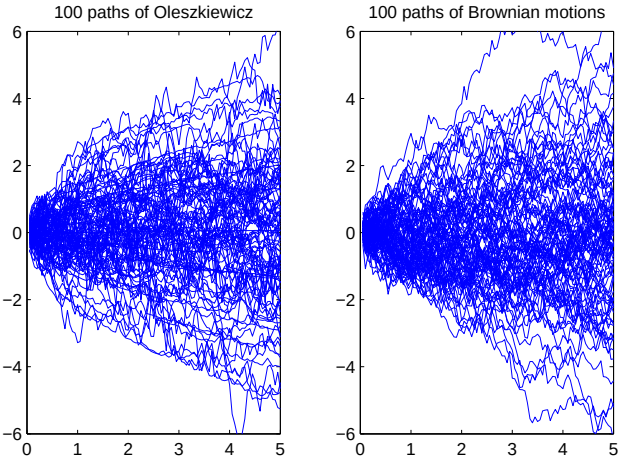

Figure 1.2: Comparison of 100 Oleszkiewicz paths and 100 Brownian motion paths: From this plot, we observe that for each time t the density of X_t and B_t are both normal.

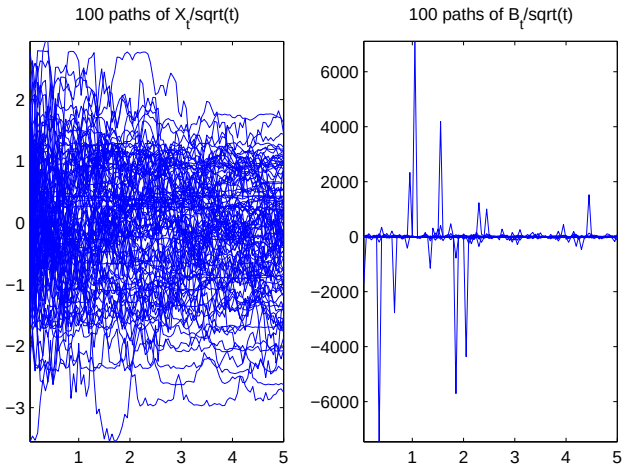

Figure 1.3: Comparison of 100 paths of $X_t^{(a)}/\sqrt{t}$ and 100 paths of $B_t/\sqrt{t}$:
From this plot, using tight axis, we find that the two processes are significantly different.

Why isn't it sufficient to take the exponential of the construction of Oleszkiewicz to obtain the fake geometric Brownian motion?

To obtain a fake geometric Brownian motion, it is not sufficient to take the exponential of the construction of Oleszkiewicz, or any construction of fake Brownian motion.

Suppose $(X_t)_{t\geqslant 0}$ is a fake Brownian motion. Consider now the process $(Y_t)_{t\geqslant 0}$ such that

$$Y_t = \exp(\sigma X_t + (r - \frac{\sigma^2}{2})t).$$

From the properties of fake Brownian motion $(X_t)_{t\geqslant 0}$, it is easy to verify that Y_t is continuous, and for every $t \geqslant 0$, Y_t follows the required log-normal distribution. However, we will prove here that $(Y_t)_{t\geqslant 0}$ cannot be a fake geometric Brownian motion.

Applying Ito's formula on $e^{-rt}Y_t$, we obtain

$$\begin{aligned}\mathrm{d}(e^{-rt}Y_t) &= e^{-rt}(-rY_t)\mathrm{d}t + e^{-rt}((r-\frac{\sigma^2}{2})Y_t\mathrm{d}t + \sigma Y_t \mathrm{d}X_t + \frac{\sigma^2}{2}Y_t \mathrm{d}\langle X, X\rangle_t) \\ &= e^{-rt}\frac{\sigma^2}{2}Y_t(\mathrm{d}\langle X, X\rangle_t - \mathrm{d}t) + e^{-rt}\sigma Y_t \mathrm{d}X_t.\end{aligned}$$

Since the fake Brownian motion X_t is a martingale, $e^{-rt}Y_t$ is a martingale if and only if $\mathrm{d}\langle X, X\rangle_t = \mathrm{d}t$. In this case, by Lévy's characterization (Theorem 1.0.1), X_t is a genuine Brownian motion. Thus we obtain a contradiction.

Hence, there is no evident way to obtain a fake geometric Brownian motion. We should consider a different form.

In the following chapters, we will drop the continuity condition in the definition of fake geometric Brownian motion, and use Skorokhod embedding method to construct non-continuous fake GBM.

Chapter 2

Skorokhod embedding

We will present, in this chapter, the solution of the Skorokhod embedding problem proposed by Azéma and Yor, to see how it can apply on our aimed marginals of geometric Brownian motion. Having applied Azéma-Yor solution and obtained the stock price paths, we will be also interested in the reversed Azéma-Yor solution.

2.1 Azéma-Yor embedding solution

2.1.1 Theory

Skorokhod embedding problem (SEP)

The Skorokhod embedding problem ([15], 1965) is as follows: given a prespecified probability measure $\mu(\mathrm{d}y)$ on $\mathbb{R}$ such that $\int |y|\mu \mathrm{d}y < \infty$ and $\int y\mu \mathrm{d}y = 0$, how to construct a stopping time τ for the standard Brownian motion B_t, such that the process of the Brownian motion stopped at the stopping time τ, i.e. B_τ, follows the distribution given by the measure μ on $\mathbb{R}$?

Azéma-Yor solution to SEP

Azéma and Yor ([2], 1979) gave a solution to this problem by constructing a barycentre function

$$\psi(x) = \frac{\int_x^\infty y\mu(\mathrm{d}y)}{\int_x^\infty \mu(\mathrm{d}y)}$$

which has the following properties:

- ψ is a positive increasing function;
- $\psi(x) \to 0$ as $x \to -\infty$;

- $\psi(x) - x \to 0$ as $x \to \infty$;
- $\psi(x) \geqslant x$.

We note M_t as the maximum to date of the Brownian motion B_t, i.e.

$$M_t = \sup_{0 \leqslant s \leqslant t} B_t,$$

and we construct the required stopping time τ as the first time the maximum to date M_t reaches the level of the barycentre function $\psi(B_t)$, i.e. τ is defined as

$$\tau = \inf \{t \geqslant 0 | M_t \geqslant \psi(B_t)\}.$$

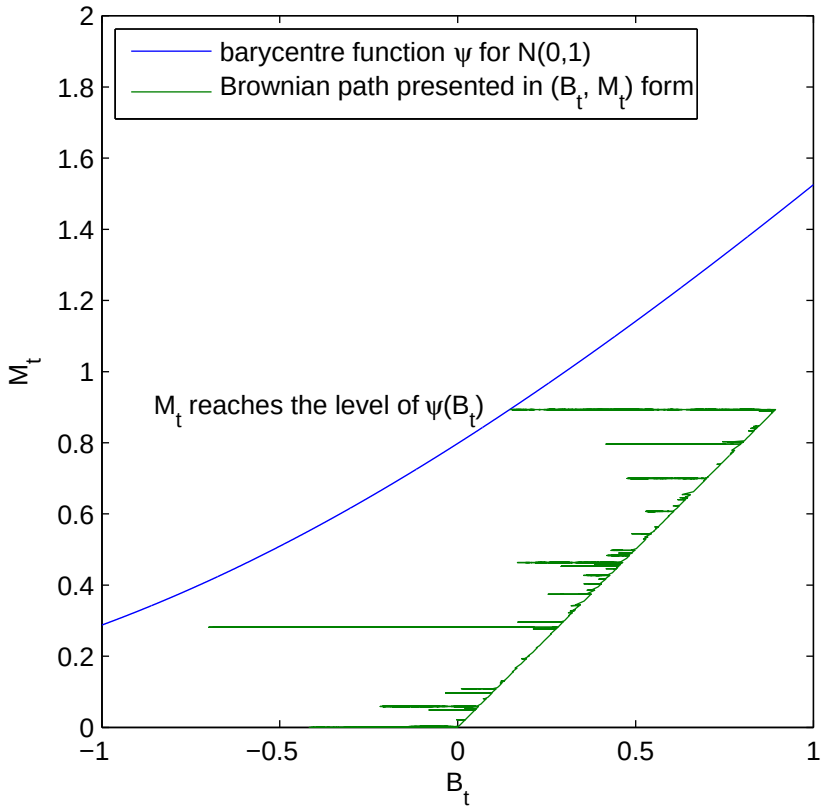

Figure 2.1: Presentation of Azéma-Yor solution for the distribution of $\mathcal{N}(0, 1)$.

In Figure 2.1, we visualize an example of Azéma-Yor solution for the distribution of $\mathcal{N}(0, 1)$. We present our Brownian path in the form of (B_t, M_t) with the green line. The path starts at $(0, 0)$. After that, it either rises along $y = x$, which means the

Brownian path climbs to a new maximum level, or moves horizontally at the left side of $y = x$. The blue line presents the barycentre function of the distribution $\mathcal{N}(0, 1)$. The stopping time stops when the green line hits the blue line for the first time. The process that we intend to construct takes B_τ, i.e. the level of the Brownian path at the first hitting time.

Extended Azéma-Yor solution for marginal densities

We can extend Azéma-Yor solution to construct martingales with prespecified marginals ([8]). Instead of considering a probability measure $\mu(\mathrm{d}y)$, we consider the marginals $\mu_t(\mathrm{d}y) = g(y, t)dy$. We suppose that

$$\int |y| g(y,t) \mathrm{d}y < \infty,$$
$$\int y g(y,t) \mathrm{d}y = 0.$$

We see that the marginals are suitable for martingales which start at 0. We define the family of barycentre functions associated with the marginals as

$$\psi_t(x) = \psi(x,t) = \frac{\int_x^\infty y g(y,t) \mathrm{d}y}{\int_x^\infty g(y,t) \mathrm{d}y}.$$

If a family of zero-expectation densities has the barycentre functions which are increasing in time t, then we say that it has the property of *increasing mean residual value* (IMRV). To construct a martingale with prespecified marginals using Azéma-Yor solution, the marginal should verify the IMRV condition.

Theorem 2.1.1. *(Madan and Yor [8]) Let $g(y, t)$ be a family of zero-expectation densities satisfying the IMRV property. Let $(B_t)_{t\geqslant 0}$ be a standard Brownian motion. There exists an increasing family of stopping times $(\tau_t)_{t\geqslant 0}$ such that:*

- *$\beta_t := B_{\tau_t}$ is a martingale;*
- *$(\beta_t)_{t\geqslant 0}$ is an inhomogeneous Markov process;*
- *For each t, the density of β_t is given by $g(y, t)$.*

To be more specified, note $M_t = \sup_{0\leqslant s\leqslant t} B_s$, and then τ_t defined by

$$\tau_t = \inf \{s \geqslant 0 | M_s \geqslant \psi(B_s, t)\}$$

is a good candidate for the family of stopping times.

Proof. See Madan and Yor, [8], 2.1.

□

2.1.2 Application on the marginals of GBM

Marginals of geometric Brownian motion

Consider the marginals of a geometric Brownian motion with volatility σ. Noting that

$$\mathbb{E}(e^{\sigma W_t - \frac{1}{2}\sigma^2 t}) = 1,$$

we shift the distribution by -1, to let the expectation be zero.

Hence, consider $Y_t = e^{\sigma Z_t - \frac{1}{2}\sigma^2 t} - 1$, where $Z_t \sim \mathcal{N}(0, t)$. We can compute the cumulative distribution function F_{Y_t}. $\forall y > -1$, we have

$$\begin{aligned} F_{Y_t}(y) &= \mathbb{P}(Y_t \leqslant y) = \mathbb{P}(e^{\sigma Z_t - \frac{1}{2}\sigma^2 t} - 1 \leqslant y) \\ &= \mathbb{P}(Z_t \leqslant \frac{1}{\sigma}(\ln(y+1) + \frac{1}{2}\sigma^2 t)) \\ &= \mathbb{P}(Z_1 \leqslant \frac{1}{\sigma\sqrt{t}}(\ln(y+1) + \frac{1}{2}\sigma^2 t)) \\ &= \Phi(\frac{1}{\sigma\sqrt{t}}(\ln(y+1) + \frac{1}{2}\sigma^2 t)), \end{aligned}$$

where Φ is the unit normal cumulative distribution function, $\Phi(d) = \int_{-\infty}^{d} \frac{1}{\sqrt{2\pi}} e^{-z^2/2} \mathrm{d}z$.

We note $g(y,t)\mathrm{d}y$ as the marginal densities for Y_t. We can deduce that $\forall y > -1$,

$$g(y,t) = F'_{Y_t}(y) = \frac{1}{\sqrt{2\pi t}} \frac{1}{\sigma(y+1)} \exp(-\frac{(\ln(y+1) + \frac{1}{2}\sigma^2 t)^2}{2\sigma^2 t}).$$

Barycentre functions ψ for GBM

Proposition 2.1.1. *The barycentre function for the marginals of geometric Brownian motion is*

$$\psi_{GBM}(x,t) = \begin{cases} \frac{\Phi((-\ln(x+1)+\frac{1}{2}\sigma^2 t)/\sigma\sqrt{t})}{\Phi((-\ln(x+1)-\frac{1}{2}\sigma^2 t)/\sigma\sqrt{t})} - 1 & \text{for } x > -1; \\ 0 & \text{otherwise.} \end{cases}$$

This function ψ_{GBM} satisfies the IMRV property.

Proof. We have the expression of $g(y,t)$. To calculate the barycentre function

$$\psi_{GBM}(x,t) = \frac{\int_x^\infty y g(y,t)\mathrm{d}y}{\int_x^\infty g(y,t)\mathrm{d}y},$$

we compute the denominator and the numerator separately.

The denominator is

$$\begin{aligned}\int_x^\infty g(y,t)\mathrm{d}y &= \mathbb{P}(Y_t \geqslant x)\\ &= \mathbb{P}(Z_t \geqslant \frac{1}{\sigma}(\ln(x+1)+\frac{1}{2}\sigma^2 t))\\ &= \mathbb{P}(Z_1 \geqslant \frac{1}{\sigma\sqrt{t}}(\ln(x+1)+\frac{1}{2}\sigma^2 t))\\ &= 1-\Phi(\frac{1}{\sigma\sqrt{t}}(\ln(x+1)+\frac{1}{2}\sigma^2 t))\\ &= \Phi(-\frac{1}{\sigma\sqrt{t}}(\ln(x+1)+\frac{1}{2}\sigma^2 t)).\end{aligned}$$

The numerator is

$$\begin{aligned}\int_x^\infty yg(y,t)\mathrm{d}y &= \int_x^\infty y\times\frac{1}{\sqrt{2\pi t}}\frac{1}{\sigma(y+1)}\exp(-\frac{(\ln(y+1)+\frac{1}{2}\sigma^2 t)^2}{2\sigma^2 t})\mathrm{d}y\\ &= \int_{\frac{1}{\sigma}(\ln(x+1)+\frac{1}{2}\sigma^2 t)}^\infty (e^{\sigma z-\frac{1}{2}\sigma^2 t}-1)\frac{1}{\sqrt{2\pi t}}e^{-z^2/2t}\mathrm{d}z\\ &= \underbrace{\int_{\frac{1}{\sigma}(\ln(x+1)+\frac{1}{2}\sigma^2 t)}^\infty e^{\sigma z-\frac{1}{2}\sigma^2 t}\frac{1}{\sqrt{2\pi t}}e^{-z^2/2t}\mathrm{d}z}_{\text{Term 1}} - \underbrace{\int_{\frac{1}{\sigma}(\ln(x+1)+\frac{1}{2}\sigma^2 t)}^\infty \frac{1}{\sqrt{2\pi t}}e^{-z^2/2t}\mathrm{d}z}_{\text{Term 2}}.\end{aligned}$$

$$\begin{aligned}\text{Term 1} &= \int_{\frac{1}{\sigma}(\ln(x+1)+\frac{1}{2}\sigma^2 t)}^\infty \frac{1}{\sqrt{2\pi t}}e^{-\frac{1}{2t}(z-\sigma t)^2}\mathrm{d}z\\ &= \int_{\frac{1}{\sigma}(\ln(x+1)-\frac{1}{2}\sigma^2 t)}^\infty \frac{1}{\sqrt{2\pi t}}e^{-\frac{1}{2t}z^2}\mathrm{d}z\\ &= \mathbb{P}(Z_t \geqslant \frac{1}{\sigma}(\ln(x+1)-\frac{1}{2}\sigma^2 t))\\ &= 1-\Phi(\frac{1}{\sigma\sqrt{t}}(\ln(x+1)-\frac{1}{2}\sigma^2 t))\\ &= \Phi(-\frac{1}{\sigma\sqrt{t}}(\ln(x+1)-\frac{1}{2}\sigma^2 t)).\end{aligned}$$

$$\text{Term 2} = \mathbb{P}(Z_t \geqslant \frac{1}{\sigma}(\ln(x+1)+\frac{1}{2}\sigma^2 t)) = \Phi(-\frac{1}{\sigma\sqrt{t}}(\ln(x+1)+\frac{1}{2}\sigma^2 t)).$$

Hence, we obtain the barycentre function for the marginals of GBM,

$$\forall x > -1, \psi_{GBM}(x,t) = \frac{\Phi(\frac{-\ln(x+1)+\frac{1}{2}\sigma^2 t}{\sigma\sqrt{t}})}{\Phi(\frac{-\ln(x+1)-\frac{1}{2}\sigma^2 t}{\sigma\sqrt{t}})} - 1.$$

For $x < -1$, we extend the function by continuity and positivity of barycentre functions.

To verify the IMRV property, we should prove that $\forall x > -1$, $\psi_{GBM}(x,t)$ is increasing in t.

$$\forall x > -1,\ t \mapsto \psi_{GBM}(x,t) = \frac{\Phi(-\frac{\ln(x+1)-\frac{1}{2}\sigma^2 t}{\sigma\sqrt{t}})}{\Phi(-\frac{\ln(x+1)+\frac{1}{2}\sigma^2 t}{\sigma\sqrt{t}})} - 1 \text{ is increasing,}$$

$$\iff \forall a \in \mathbb{R},\ t \mapsto \frac{\Phi(-\frac{1}{\sigma\sqrt{t}}(a-\frac{1}{2}\sigma^2 t))}{\Phi(-\frac{1}{\sigma\sqrt{t}}(a+\frac{1}{2}\sigma^2 t))} \text{ is increasing,}$$
(as the function $x \mapsto \ln(x+1)$ is surjective from $(-1,+\infty)$ to $\mathbb{R}$.)

$$\iff \forall a \in \mathbb{R},\ t \mapsto \frac{\Phi(\frac{1}{2\sigma\sqrt{t}}(a+\sigma^2 t))}{\Phi(\frac{1}{2\sigma\sqrt{t}}(a+\sigma^2 t))} \text{ is increasing,}$$
(as the function $a \mapsto -2a$ is surjective from $\mathbb{R}$ to $\mathbb{R}$.)

$$\iff \forall a \in \mathbb{R},\ t \mapsto \frac{\Phi(\frac{a+t}{2\sqrt{t}})}{\Phi(\frac{a-t}{2\sqrt{t}})} \text{ is increasing,}$$
(as the function $t \mapsto \sigma^2 t$ is increasing and surjective from $\mathbb{R}_+$ to $\mathbb{R}_+$.)

We note $f(a,t) := \frac{\Phi((a+t)/2\sqrt{t})}{\Phi((a-t)/2\sqrt{t})}$. We will prove in the following that $\forall a \in \mathbb{R},\ t \mapsto f(a,t)$ is increasing.

$$\begin{aligned}\frac{\partial f}{\partial t}(a,t) = \frac{1}{(\Phi((a-t)/2\sqrt{t}))^2}\Big(&\frac{1}{\sqrt{2\pi}}e^{-(\frac{a+t}{2\sqrt{t}})^2/2} \times \frac{t-a}{4t\sqrt{t}} \times \Phi(\frac{a-t}{2\sqrt{t}}) \\ &- \frac{1}{\sqrt{2\pi}}e^{-(\frac{a-t}{2\sqrt{t}})^2/2} \times \frac{-t-a}{4t\sqrt{t}} \times \Phi(\frac{a+t}{2\sqrt{t}})\Big)\end{aligned}$$

$$= \frac{1}{4t\sqrt{2\pi t}}e^{-\frac{1}{8t}(a+t)^2}\underbrace{\Big((t-a)\Phi(\frac{a-t}{2\sqrt{t}}) + e^{\frac{a}{2}}(t+a)\Phi(\frac{a+t}{2\sqrt{t}})\Big)}_{=:\mathrm{h(t,a)}}$$

In the following, we would like to verify that

$$\forall (a,t) \in \mathbb{R} \times \mathbb{R}_+,\ h(t,a) \geqslant 0.$$

In fact, $\forall a$,

$$\begin{aligned}\frac{\partial h}{\partial t}(t,a) &= \Phi(\frac{a-t}{2\sqrt{t}}) + (t-a) \times \frac{1}{\sqrt{2\pi}} e^{-(\frac{a-t}{2\sqrt{t}})^2/2} \times \frac{-t-a}{4t\sqrt{t}} \\ &\quad + e^{\frac{a}{2}}\Phi(\frac{a+t}{2\sqrt{t}}) + e^{\frac{a}{2}}(t+a) \times \frac{1}{\sqrt{2\pi}} e^{-(\frac{a+t}{2\sqrt{t}})^2/2} \times \frac{t-a}{4t\sqrt{t}} \\ &= \Phi(\frac{a-t}{2\sqrt{t}}) + e^{\frac{a}{2}}\Phi(\frac{a+t}{2\sqrt{t}}) \\ &> 0.\end{aligned}$$

When $a > 0$, $\Phi(\frac{a-t}{2\sqrt{t}})$ and $\Phi(\frac{a+t}{2\sqrt{t}})$ tend to 1 as t tends to 0. We have

$$h(a,t) \to a(e^{\frac{a}{2}} - 1) > 0, \text{ as } t \to 0.$$

When $a \leqslant 0$, $\Phi(\frac{a-t}{2\sqrt{t}})$ and $\Phi(\frac{a+t}{2\sqrt{t}})$ tend to 0 as t tends to 0. We have

$$h(a,t) \to 0, \text{ as } t \to 0.$$

Thus, $\forall a \in \mathbb{R}$, $h(t,a)$ is increasing in t, and $\lim_{t\to 0} h(a,t) \geqslant 0$. $h(a,t)$ is indeed positive for all $(a,t) \in \mathbb{R} \times \mathbb{R}_+$.

Hence, $f(a,t)$ is increasing in t, and we conclude that the barycentre function $\psi_{GBM}(x,t)$ is also increasing in t, and satisfies the IMRV property.

□

Corollary 2.1.1. *We note τ_t as the increasing family of stopping times*

$$\tau_t = \inf\{s \geqslant 0 | M_s \geqslant \psi_{GBMt}(B_s)\}.$$

Then $S_t^{AY} := S_0 e^{rt}(B_{\tau_t} + 1)$ has the same marginals as

$$S_0 \exp(\sigma Z_t + (r - \frac{\sigma^2}{2})t), \text{ where } Z_t \sim \mathcal{N}(0,t).$$

And the discounted process $(e^{-rt}S_t^{AY})_{t\geqslant 0}$ is a martingale.

In the following parts of the thesis, we call the process (S_t^{AY}) *Azéma-Yor fake GBM*, and use it as one stock price.

Proof. Using Theorem 2.1.1 and Proposition 2.1.1, it is easy to come to the conclusion.

□

Remark 2.1.1. When using Theorem 2.1.1, we shift the marginals to obtain a martingale with zero expectation. It is also possible to leave the martingale starting at 1. Then the barycentre function becomes

$$\psi'_{GBM}(x,t) = \begin{cases} \frac{\Phi((-\ln x + \frac{1}{2}\sigma^2 t)/\sigma\sqrt{t})}{\Phi((-\ln x - \frac{1}{2}\sigma^2 t)/\sigma\sqrt{t})} & \text{for } x > 0; \\ 1 & \text{otherwise,} \end{cases}$$

and instead of simulating with the standard Brownian motion which starts at 0, we should use a Brownian motion which starts at 1.

A general view of path generation

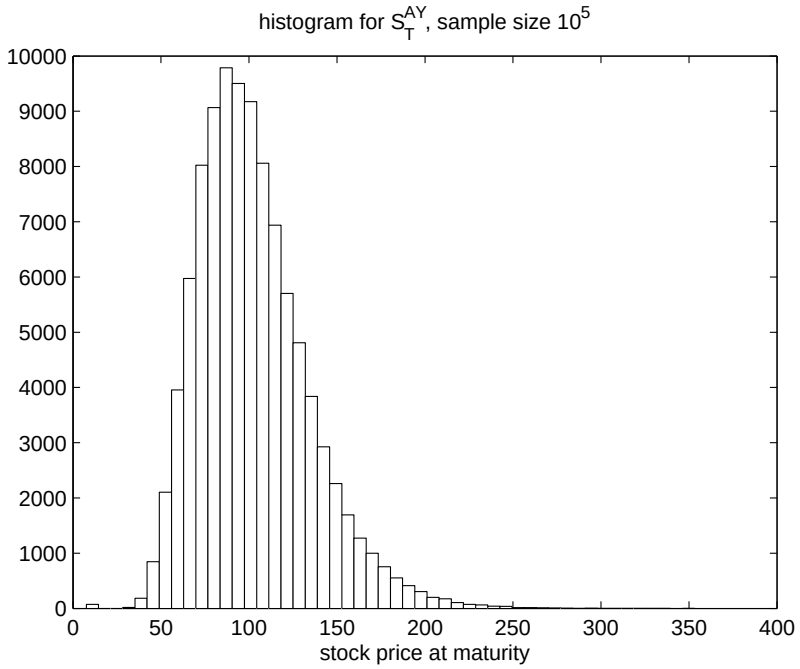

Figure 2.2: Example: histogramme of S_T^{AY}. $S_0 = 100$, $T = 1$, $r = 0.02$, $\sigma = 0.3$.

In Figure 2.2, the stock prices at maturity of Azéma-Yor fake GBM are generated with a sample size of 10^5. We find that the distribution has indeed a log-normal shape. It is also valid for stock prices at anytime t between 0 and T.

In Figure 2.3, three paths of Azéma-Yor fake GBM are plotted. It is obviously different from stock prices following the classical geometric Brownian motion. While the marginals are the same, the joint distributions are significantly different. Thus,

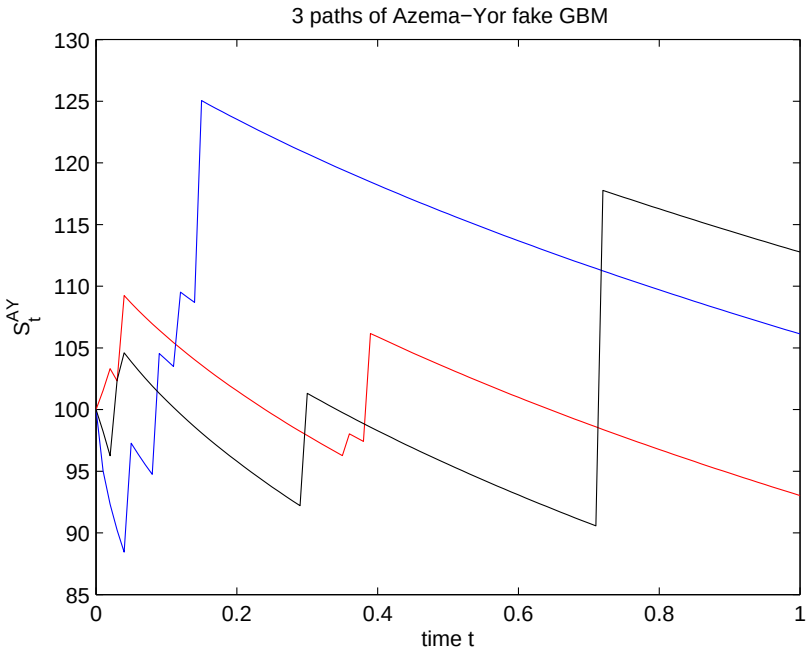

Figure 2.3: 3 paths of Azéma-Yor fake GBM.

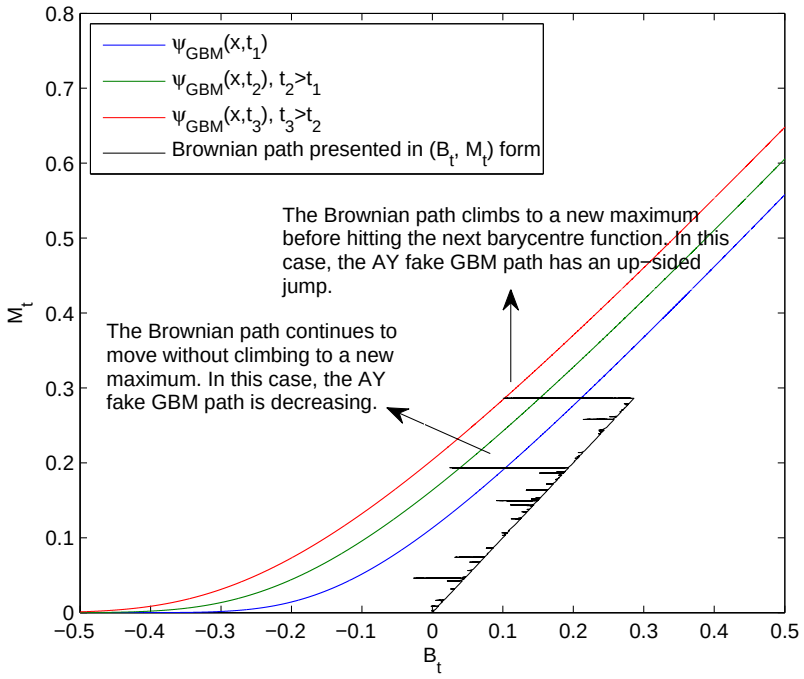

Figure 2.4: Explanation: why Azéma-Yor fake GBM path is either continuously decreasing or has an up-sided jumping?

clearly by the plots, we see that we construct a fake geometric Brownian motion process without satisfying the continuity condition.

We observe that these paths are quite interesting: they are continuously decreasing, except where some up-sided jumps occur. This kind of appearance can be explained intuitively by Figure 2.4.

The pattern of Azéma-Yor fake GBM paths is quite opposite to what happens in the real world, which leads us to consider trying another Skorokhod embedding solution – the reversed Azéma-Yor solution.

2.2 Reversed Azéma-Yor embedding solution

2.2.1 Theory

The reversed Azéma-Yor embedding solution ([9]) is similar to the Azéma-Yor embedding solution. Instead of using the barycentre function ψ for the desired marginals, and the maximum to date M_t for the Brownian motion, we use a "downside" barycentre function Θ and the minimum to date $\tilde{M}_t$. They are defined by

$$\begin{cases} \Theta(x,t) = \dfrac{\int_{-\infty}^{x} y g(y,t)\mathrm{d}y}{\int_{-\infty}^{x} g(y,t)\mathrm{d}y}, \\ \tilde{M}_t = \inf\limits_{0\leqslant s\leqslant t} B_t. \end{cases}$$

Theorem 2.2.1. *Let $g(y,t)$ be a family of zero-expectation densities of which the downside barycentre function Θ is decreasing in time. Let $(B_t)_{t\geqslant 0}$ be a standard Brownian motion. There exists an increasing family of stopping times $(\tilde{\tau}_t)_{t\geqslant 0}$ such that:*

- *$\tilde{\beta}_t := B_{\tilde{\tau}_t}$ is a martingale;*
- *$(\tilde{\beta}_t)_{t\geqslant 0}$ is an inhomogeneous Markov process;*
- *For each t, the density of $\tilde{\beta}_t$ is given by $g(y,t)$.*

To be more specified, note $\tilde{M}_t = \inf_{0\leqslant s\leqslant t} B_s$, and then $\tilde{\tau}_t$ defined by

$$\tilde{\tau}_t = \inf\{s \geqslant 0 | \tilde{M}_s \leqslant \Theta(B_s, t)\}$$

is a good candidate for the family of stopping times.

Proof. The same argument allows us to prove this theorem as Theorem 2.1.1.

□

2.2.2 Application on the marginals of GBM

Downside barycentre function Θ for GBM

Proposition 2.2.1. *The downside barycentre function for the marginals of geometric Brownian motion is*

$$\Theta_{GBM}(x,t) = \begin{cases} \frac{\Phi((\ln(x+1)-\frac{1}{2}\sigma^2 t)/\sigma\sqrt{t})}{\Phi((\ln(x+1)+\frac{1}{2}\sigma^2 t)/\sigma\sqrt{t})} - 1 & \text{for } x > -1; \\ -1 & \text{otherwise.} \end{cases}$$

The downside barycentre function Θ_{GBM} is decreasing in t.

Proof. Using the same techniques as for Proposition 2.1.1, we can compute $\Theta_{GBM}(x,t)$ easily.

To prove $\forall x > -1$, $t \mapsto \Theta_{GBM}(x,t)$ is decreasing, it is equivalent to prove that $\forall a \in \mathbb{R}$, $t \mapsto \frac{\Phi((a-t)/2\sqrt{t})}{\Phi((a+t)/2\sqrt{t})}$ is decreasing, which is true since we have already demonstrated that the reciprocal $t \mapsto f(a,t)$ is increasing.

□

Corollary 2.2.1. *We note $\tilde{\tau}_t$ as the increasing family of stopping times*

$$\tilde{\tau}_t = \inf\{s \geqslant 0 | \tilde{M}_s \leqslant \Theta_{GBMt}(B_s)\}.$$

Then $S_t^{RevAY} := S_0 e^{rt}(B_{\tilde{\tau}_t} + 1)$ has the same marginals as

$$S_0 \exp(\sigma Z_t + (r - \frac{\sigma^2}{2})t), \text{ where } Z_t \sim \mathcal{N}(0,t).$$

And the discounted process $(e^{-rt}S_t^{RevAY})_{t\geqslant 0}$ is a martingale.

In the following parts, we call the process (S_t^{RevAY}) *reversed Azéma-Yor fake GBM*, and use it as another stock price.

Proof. Using Theorem 2.2.1 and Proposition 2.2.1, it is easy to come to the conclusion.

□

A general view of path generation

We generate some paths of stock price using the reversed Azéma-Yor fake GBM. The paths are continuously increasing, except where some down-sided jumps occur. This can be explained by similar arguments as for the Azéma-Yor fake GBM paths. We see that the paths have different patterns from stock prices following the classical geometric Brownian motions. They have different joint distributions.

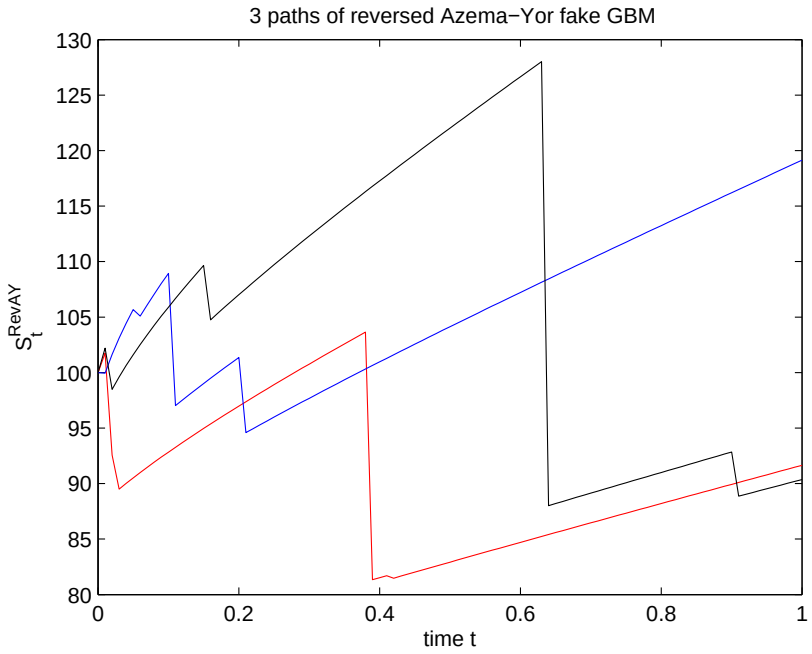

Figure 2.5: 3 paths of reversed Azéma-Yor fake GBM.

Chapter 3

Numerical considerations

From the previous chapter, we have obtained two theoretical methods to generate discontinuous fake geometric Brownian motions. Our purpose is to generate a large sample of stock prices following these two fake processes, and then use Monte Carlo method to price both European and path-dependent options, with such underlying stocks. In this case, how to approach these processes as accurate as possible, under the constraint of computing cost limitation, deserves to attract our attention.

In this chapter, we will discuss some numerical considerations for the simulation. We will at first look at how to generate the stock prices at one specific moment, such as the maturity, and then investigate the generation of the whole path.

Since the implementation of the two processes is similar, we will only take Azéma-Yor fake GBM as an example in the following.

3.1 Stock prices at maturity

3.1.1 Generation of S_T without using Brownian bridge

We have to discretisize our Brownian paths correctly in order to stop at the first time the maximum to date of the Brownian motion climbs up to the level of the barycentre function.

1) Level of the Brownian path timestep

We define N as the level of the Brownian path timestep such that the discretisized timestep $\mathrm{dt} = \mathrm{T}/10^{\mathrm{N}}$. In our specific case where we are simulating in order to find the stopping time, dt must be small enough; otherwise, if we miss the first time M_t hits the barycentre function, then it is possible that the result would be totally different. However, from the pseudo-code of Table 3.1, we see that increasing N

Table 3.1: Pseudo-code for generating one sample of S_T

Mark	Pseudo-code
	Define Brownian path timestep level N s.t. dt = T/10^{N}
	$B \leftarrow 0$, $M \leftarrow 0$ `% at time 0`
$(\star)$	*while* $M < \psi_{GBM_T}(B)$
	$B \leftarrow B + \sqrt{\mathrm{dt}} \times Z$ `% Z follows N(0,1)`
	$M \leftarrow \max(B, M)$ `% at time t+dt`
	end while
	$B \leftarrow \psi^{-1}_{GBM_T}(M)$
	$S_T \leftarrow S_0 e^{rT}(B + 1)$

requires large computational capacity. For generating even one sample, the number of *while* loops is proportional to 10^N. Thus, we should find a compromise for N between our requirement of approximation and the limitation of computational capacity.

Here, we use $N = 5$. In this case, the standard deviation $\sqrt{\mathrm{dt}} \approx 0.003$ for each increment. From our numerical experiments, a large number of samples using the level $N = 5$ behave quite well.

2) Excessive occurrence for some extreme values

The histogram of stock prices at maturity via Azéma-Yor solution (Figure 3.1) shows that S_T^{AY} does follow the log-normal distribution. Furthermore, in Figure 3.2, we see that the cumulative distribution functions for S_T^{AY} and $S_T^{B\&S}$ coincide with each other with some slight difference.

However, in the histogram, we observe that there is a high occurence of value at 8, which corresponds to the stopped Brownian motion at level $B_{\tau_T} = -0.92$. Calculating $\psi_{GBM_T}(B_{\tau_T})$ on $B_{\tau_T} = -0.91$ and $B_{\tau_T} = -0.92$, we get

$$\begin{cases} \psi_{GBM_{T=1}}(-0.91) = 2.3759 \times 10^{-14}, \\ \psi_{GBM_{T=1}}(-0.92) = 0. \end{cases}$$

Here we see that, due to the limitation of machine precision, $\psi_{GBM}(B_{\tau_T}, T)$ for $T = 1$ hits 0 when B_{τ_T} is near -0.92. However, in analytical form, it is strictly positive for $B_{\tau_T} > -1$. A certain amount of Brownian paths, which never pass 0 as maximum,

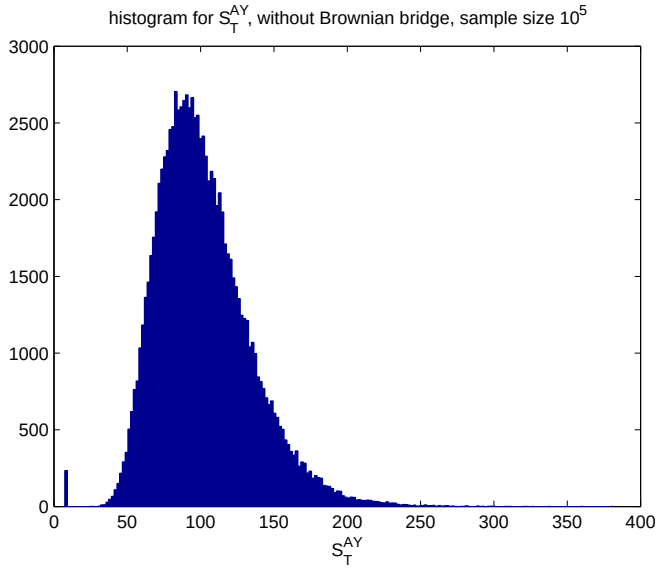

Figure 3.1: Histogram of stock price at maturity S_T^{AY}, without using Brownian bridge. The stock prices at maturity follow the log-normal distribution. However, there is an apparent singleton of value at 8.

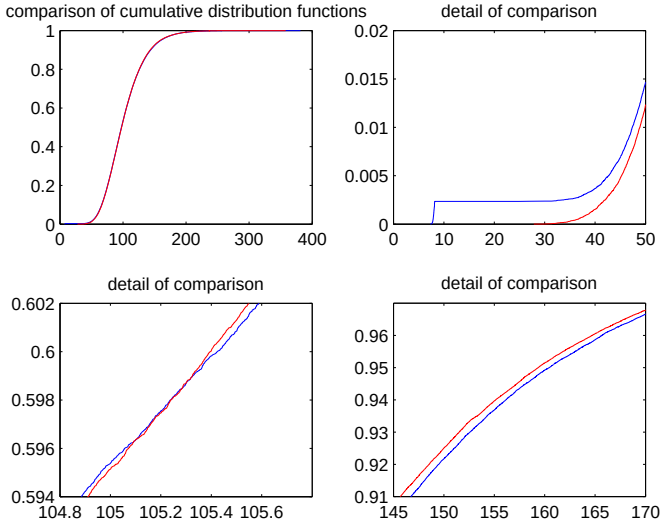

Figure 3.2: Comparison of cumulative distribution functions for stock prices at maturity. The red line is plotted for the *cdf* of $S_T^{B\&S}$; the blue one is plotted for the *cdf* of S_T^{AY} without using Brownian bridge. In the first overview plot, we see that the two *cdf* concide with each other very closely. We can observe the difference from the other three zooms. The blue line is slightly higher for the stock price range $[0, 105]$ and then the red line exceeds the blue line for bigger stock prices.

stop at -0.92. That is the reason for which there is a singleton of bin around the value 8 for the stock price at maturity.

Similarly, for the reversed Azéma-Yor solution, there is a singleton of bin at value 1274, which is also caused by the limitation of machine precision when computing the extremely small output of $\Theta_{GBM}(B_{\tau_T}, T)$.

In fact, $M_t = 0$ will never happen in theory. $\forall t > 0$, $\mathbb{P}(M_t > 0) = 1$. But it does happen for the numerical discretization. We try to solve this problem by imposing $M > 0$. In the pseudo-code of Table 3.1, for the asterisk line, instead of *while* $M < \psi_{GBM_T}(B)$, we try *while* $M < \psi_{GBM_T}(B)$ or $M = 0$. However, the new result shows that imposing $M > 0$ leads lack of downside data and is not suitable as well. In this case, we may use a Brownian bridge for each timestep of the Brownian path.

3.1.2 Generation of S_T using Brownian bridge

We implement a function `[dB,dMax,dMin]=Bridge(dt,n)`. Using this function, we generate a Brownian bridge path from time 0 to time dt, with 2^n points generated on the path. The outputs `dB`, `dMax`, and `dMin` represent the value of the Brownian motion on the end of the bridge path, the maximum on the bridge path, and the minimum after the maximum has occurred. For example, using $n = 3$ in our simulation, if the generated bridge path is

$$-0.0001 \quad -0.0008 \quad -0.0001 \quad -0.0002 \quad 0.0005 \quad -0.0016 \quad -0.0038 \quad -0.0027,$$

then the outputs `dB`, `dMax`, `dMin` are -0.0027, 0.0005, and -0.0038 respectively.

From Table 3.2, we present our pseudo-code for generating one sample of stock price using Brownian bridge for each timestep. The stock prices generated via such a method show some improvement in the histogram. From Figure 3.3, we see that though there is still the singleton of bin at value 8 due to the limitation of machine precision, the bin becomes much lower. Less paths are stopped in the case where the maximum to date M_t never exceeds 0. We plot the cumulative distribution function to verify that generally it behaves well, too.

Note that for the reversed Azéma-Yor solution, we should implement another bridge function to output the minimum on the bridge path, and the maximum after the minimum has occurred.

Table 3.2: Pseudo-code for generating one sample of S_T using Brownian bridge

Mark	Pseudo-code
	Define Brownian path timestep level N s.t. $\mathrm{dt} = \mathrm{T}/10^{\mathrm{N}}$
	$[\mathrm{B}, \mathrm{Max}, \mathrm{Min}] \leftarrow \mathrm{Bridge}(\mathrm{dt}, \mathrm{n})$, $\mathrm{Max} \leftarrow \max(\mathrm{Max}, 0)$ `% at time 0`
	while $\mathrm{Max} < \psi_{GBM_T}(\mathrm{Min})$
	$[\mathrm{dB}, \mathrm{dMax}, \mathrm{dMin}] \leftarrow \mathrm{Bridge}(\mathrm{dt}, \mathrm{n})$
	$\mathrm{Max} \leftarrow \max(\mathrm{B} + \mathrm{dMax}, \mathrm{Max})$
	$\mathrm{Min} \leftarrow \mathrm{B} + \mathrm{dMin}$
	$\mathrm{B} \leftarrow \mathrm{B} + \mathrm{dB}$ `% at time t+dt`
	end while
	$\mathrm{B} \leftarrow \psi^{-1}_{GBM_T}(\mathrm{Max})$
	$S_T \leftarrow S_0 e^{rT}(\mathrm{B} + 1)$

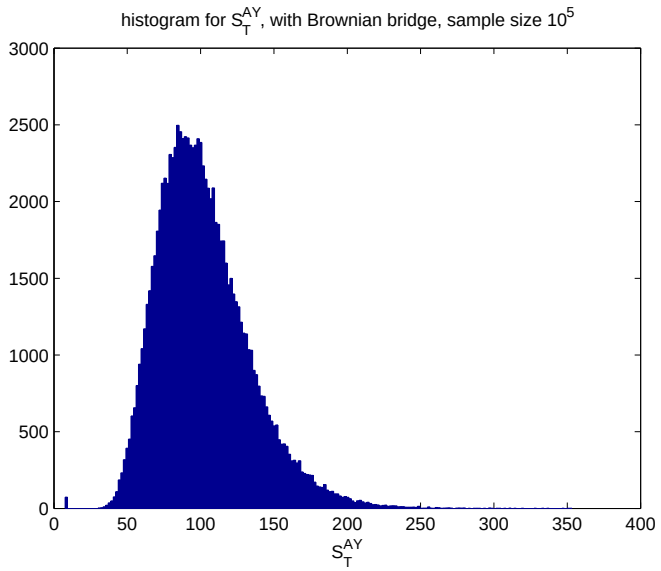

Figure 3.3: Histogram of stock price at maturity S_T^{AY}, with using Brownian bridge. There is still the singleton at value 8, but with much smaller occurrence.

In the following, for generating Azéma-Yor fake GBM paths, we will continue using the Brownian bridge technique.

3.2 Stock price paths

We studied how to generate the stock prices for one fixed time in the previous section. Here for each moment t between 0 and T, we should generate associated stock price, and thus obtain a whole Azéma-Yor fake GBM path on the horizon $[0, T]$.

1) Notice on the simulated Brownian paths and the stopping times

In our construction, it is the most essential that for generating Azéma-Yor fake GBM points for different moments on the same path, we should compute the family of stopping times $(\tau_t)_{0\leqslant t\leqslant T}$ stopped on the **same** Brownian path.

Nevertheless, we recall that the family of the stopping times is increasing. Using this property, the code could be quite straightforward, and the computational cost is enormously reduced.

Table 3.3: Pseudo-code for generating one AY fake GBM path using Brownian bridge

Mark	Pseudo-code
	Define stock price path timestep level P s.t. $\mathrm{dT} = \mathrm{T}/10^{\mathrm{P}}$
	Define Brownian path timestep level N
	Reset $\mathrm{N} \leftarrow \max(\mathrm{N}, \mathrm{P})$, and set $\mathrm{dt} \leftarrow \mathrm{T}/10^{\mathrm{N}}$
	$S(0) \leftarrow S_0$
	$[\mathrm{B}, \mathrm{Max}, \mathrm{Min}] \leftarrow \mathrm{Bridge}(\mathrm{dt}, \mathrm{n})$, $\mathrm{Max} \leftarrow \max(\mathrm{Max}, 0)$
	for i from 1 to 10^P
	$t \leftarrow i \times T/10^P$
	while $\mathrm{Max} < \psi_{GBM}(\mathrm{Min}, t)$
	$[\mathrm{dB}, \mathrm{dMax}, \mathrm{dMin}] \leftarrow \mathrm{Bridge}(\mathrm{dt}, \mathrm{n})$
	$\mathrm{Max} \leftarrow \max(\mathrm{B} + \mathrm{dMax}, \mathrm{Max})$
	$\mathrm{Min} \leftarrow \mathrm{B} + \mathrm{dMin}$
	$\mathrm{B} \leftarrow \mathrm{B} + \mathrm{dB}$
	end while
$(\star)$	$\mathrm{B'} \leftarrow \psi^{-1}_{GBM_t}(\mathrm{Max})$
	$S(i) \leftarrow S_0 e^{rt}(\mathrm{B'} + 1)$
	end for

2) Relationship between choosing timestep for the Brownian path and the timestep for the AY fake GBM path

We define P as the level of the Azéma-Yor fake GBM path timestep such that we compute evenly $(10^P + 1)$ points on the horizon $[0, T]$. From our construction, it is obvious to see that the level of the Brownian path timestep N should be equal to or smaller than P. Our experiment on the simulation shows that $N = P + 3$ is a good choice for the pair of (N, P). If $N < P + 3$, the paths cannot be smooth enough; if $N > P + 3$, larger and unnecessary computational costs are required.

In our simulation, we use $N = 5$ and $P = 2$. Note that the stock price path timestep $T/100$ might not be small enough for pricing the path-dependent options with traditional underlying stock price following GBM, but is sufficient for the AY fake GBM paths as they have some particular regularity.

3) Smoothness

We notice from the pseudo-code in Table 3.3 that instead of using the value of the Brownian motion at the stopped step, we solve the equation $\{B' | M_{\tau_t} = \psi_{GBM}(B', t)\}$ for the marked asterisk line. This equality holds a.s. due to the continuity of the Brownian motion path, and the continuity and strict monotonicity of the barycentre function. In fact, it is not necessary to solve this equation for generating prices at maturity, since the interval where the stopped Brownian motion could be located for the step is small enough and will not change the distribution to a noticeable extent. However, for generating the paths, using this technique will make the paths become much smoother[1].

[1]The smoothness can help to reduce the error when simulating κ for variance swap in the next chapter.

Chapter 4

Option pricing

Having obtained our maturity and path generation in the previous chapter, we will, in this chapter, study in the option pricing by Monte Carlo method using these data. We will see that for European options, the stock prices via Azéma-Yor and reversed Azéma-Yor fake GBM result in the same price as indicated by the famous Black & Scholes formula. However, some differences appear when we price the path-dependent options.

4.1 European call option

We compute European call option price, for which the payoff at maturity T is defined by $(S_T - K)^+$. By risk neutral valuation, the price at time 0 is

$$C_0^{euro} = e^{-rT}\mathbb{E}^{\mathbb{Q}}((S_T - K)^+|\mathcal{F}_0).$$

We find that this call option price depends only on the stock price at maturity, in which case our Azéma-Yor and reversed Azéma-Yor fake GBM have the same log-normal distribution as the stock prices following the classical geometric Brownian motion. Therefore *a priori* the European call option prices should be the same. We compute the option prices for our two processes via Monte Carlo method, and compare them with the classical Black & Scholes formula.

From Figure 4.1 which plots the prices for strike K from 0 to 250, we see that the two prices via our fake processes are very close to the one of Black and Scholes. In this case, we plot the absolute differences and the relative differences in Figure 4.2. The slight differences for the prices are due to some simulation differences which can be explained by the cumulative distribution function in Figure 3.2. However, for both the two fake processes, the absolute differences are far less than 1% for strikes reasonably ranging from 50 to 150. Hence, we conclude that our simulation results in a good approximation.

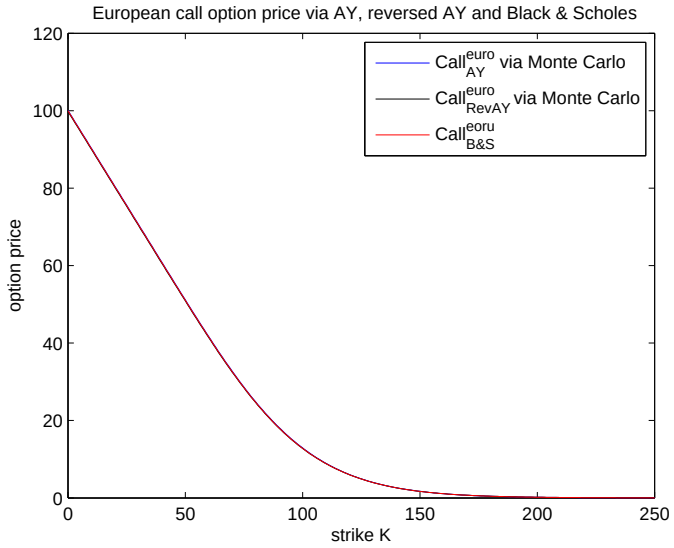

Figure 4.1: Comparison of European call option prices for different strikes K via Azéma-Yor fake GBM, reversed Azéma-Yor fake GBM, and Black & Scholes formula. The Monte Carlo sample sizes for the first two are both 10^5.

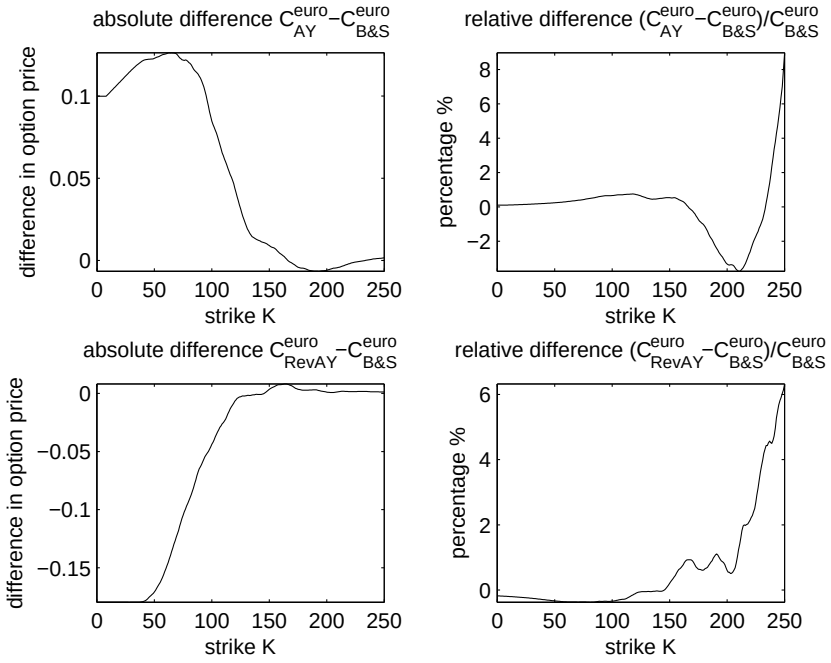

Figure 4.2: The absolute and relative differences between the simulated European call option prices via the two processes and the explicit price via Black & Scholes formula.

4.2 One-touch option

One-touch option is one kind of barrier option which pays at maturity T

$$\mathbf{1}_{\{\max_{0\leqslant t\leqslant T} S_t \geqslant B\}}$$

where B is the predetermined barrier. It is also called up-and-in digital option. By risk neutral valuation, its price at time 0 is

$$D_0^{UI} = e^{-rT}\mathbb{E}^{\mathbb{Q}}(\mathbf{1}_{\{\max_{0\leqslant t\leqslant T} S_t \geqslant B\}}|\mathcal{F}_0) = e^{-rT}\mathbb{Q}(\mathbf{1}_{\{\max_{0\leqslant t\leqslant T} S_t \geqslant B\}}|\mathcal{F}_0).$$

Under Black and Scholes setting, we can compute the density function of the maximum on path, and thus, this one-touch option has an explicit form ([14]) for the price which equals to

$$D_{B\&S0}^{UI} = e^{-rT}(\Phi(\frac{-m+\delta T}{\sqrt{T}}) + e^{2\delta m}\Phi(\frac{-m-\delta T}{\sqrt{T}}))$$

for $B > S_0$, where $\delta = \frac{r-\sigma^2/2}{\sigma} = r/\sigma - \sigma/2$ and $m = \frac{1}{\sigma}ln(B/S_0)$.

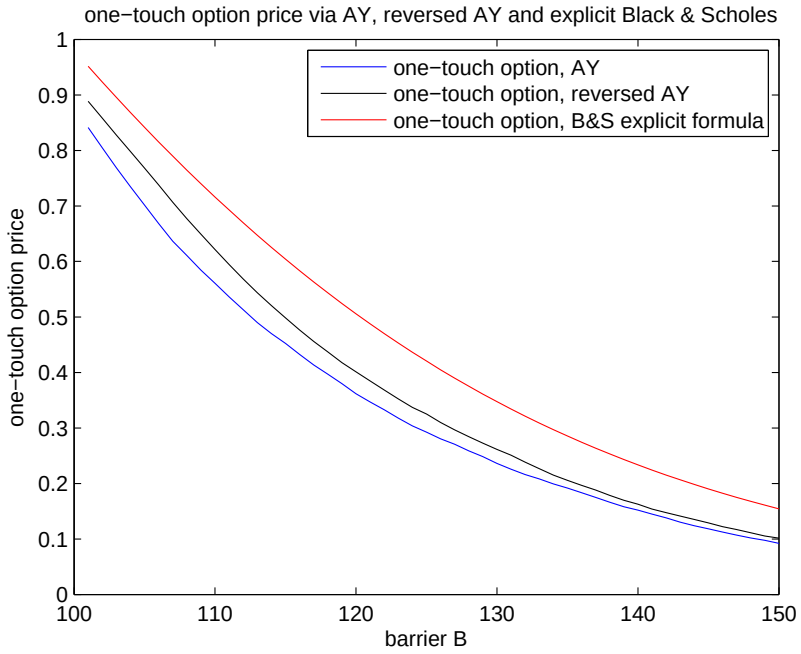

Figure 4.3: The prices of one-touch option for barrier B from 100 to 150, via Azéma-Yor fake GBM, reversed Azéma-Yor fake GBM, and Black & Scholes. The Monte Carlo sample sizes for the first two are both 10^4.

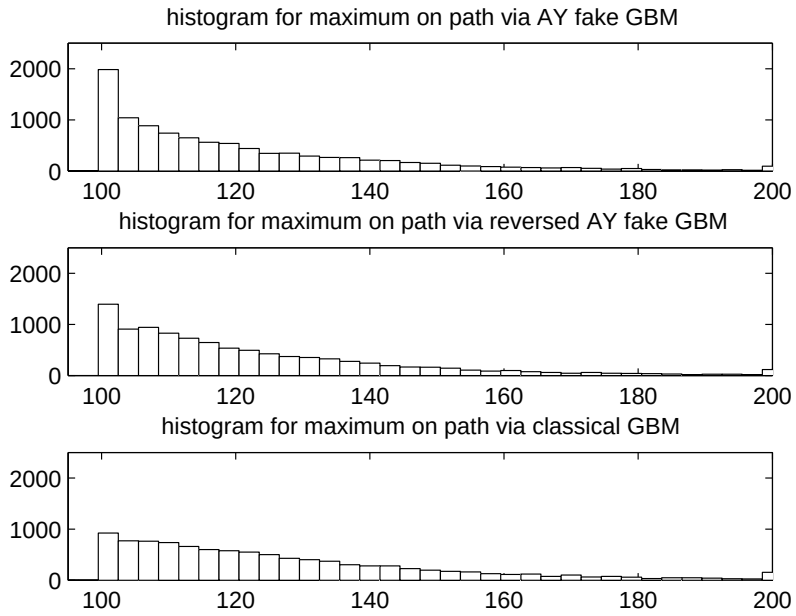

Figure 4.4: Histograms of the maximum on path for the three processes. Each of the three has 10^4 as the sample size. Here, the classical GBM paths are generated by forward Euler-Maruyama scheme.

We compute by Monte Carlo method the option prices via our two constructed processes, and compare them with the explicit Black and Scholes price. From Figure 4.3, we observe that the one-touch price for the classical GBM stock price is higher than the other two by about 0.1, which means, with the discounted factor taken into account, on average, the probability that the maximum on path exceeds the barrier for the classical GBM is 10% higher than the other two. As it is hard, or even not likely, to derive an explicit form for the distribution of the maximum on path for the two fake processes due to the particular contruction method, we try to find some reasons via the histograms. From Figure 4.4, we see that there are more paths which never exceed the initial stock price S_0, which is in our simulation, equal to 100 for the two constructed processes than the classical GBM stock prices. They contribute to the low prices for these two processes.

From the one-touch option, we conclude that the distributions of the maximum on path are different for fake processes and the classical geometric Brownian motion.

4.3 Asian option

Here, we study the fixed-strike Asian call option which pays at maturity

$$(\frac{1}{T}\int_0^T S_t \mathrm{dt} - K)^+.$$

Its price at time 0 is

$$C_0^{Asian} = e^{-rT}\mathbb{E}^{\mathbb{Q}}((\frac{1}{T}\int_0^T S_t \mathrm{dt} - K)^+ | \mathcal{F}_0).$$

The price of Asian option is not known as a closed form even under the B&S setting. Hence, we compute the prices for the three processes by Monte Carlo simulation.

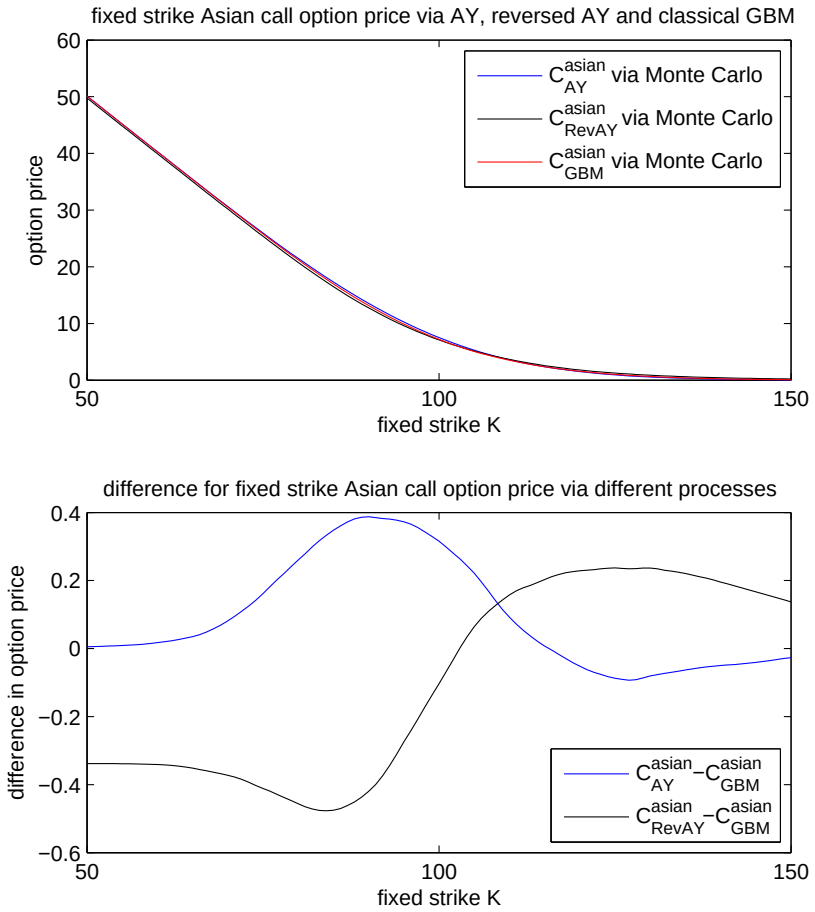

Figure 4.5: The prices and their differences of fixed-strike Asian call option for strike K from 50 to 150, via Azéma-Yor fake GBM, reversed Azéma-Yor fake GBM, and classical GBM. The Monte Carlo sample size is 10^4.

It is somehow surprising to see, from Figure 4.5, that the prices of the fixed-strike Asian call option for the two fake processes are nearly the same as the one under Black & Scholes setting.

To do some further analysis, we plot the histogram of the path average for the three processes, and find that the distributions of the average are actually not the same. It is clear to see, in Figure 4.6, that for the path average via reversed AY fake GBM, the distribution has a lower centralized peak compared to the one of the classical GBM, which could have cut down the Asian call option price. However, more extremly-high-average events take place and compensate the former impact. Similarly but with less clarity on the plot, the distribution of the path average via AY fake GBM has a higher centralized peak compared to the one under B&S setting, but with more downside average events which take place.

For Asian options, we find that although the option prices are close for the three processes, the distributions of the path average are different.

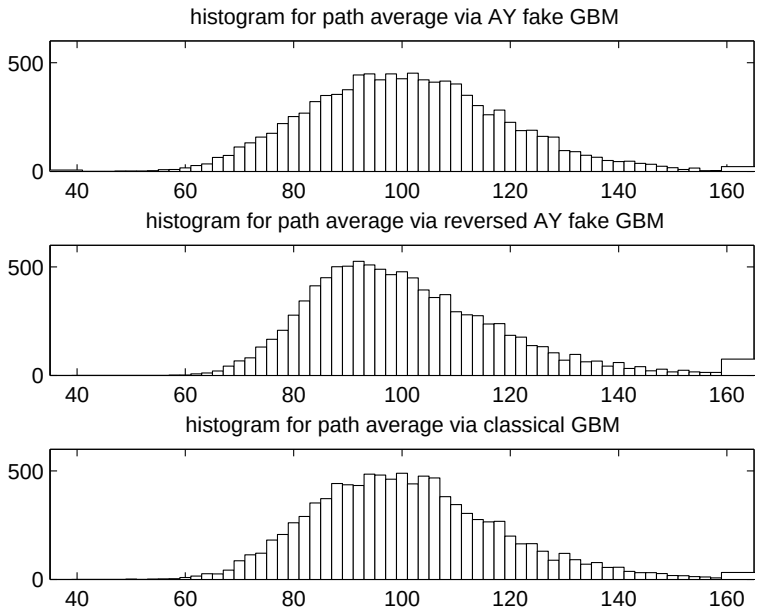

Figure 4.6: Histograms of the path average for the three processes.

4.4 Variance swap

A variance swap ([10]) is a contract with payoff at maturity

$$[X]_T - \kappa_{var},$$

where $X_t = \ln(S_t/S_0)$ and $[X]_t$ is the quadratic variation of (X_t). The constant κ_{var} is predetermined in order that there is no cash flow when the contract is set.

Under the Black & Scholes setting, κ_{var} can be computed and equal to $\sigma^2 T$.

For our fake GBM processes, we approach κ_{var} by computing for a large N

$$\sum_{i=0}^{N-1} (X_{t_{i+1}} - X_{t_i})^2 = \sum_{i=0}^{N-1} (\ln \frac{S_{t_{i+1}}}{S_{t_i}})^2$$

for each path and then get the result via Monte Carlo simulation.

Hence, we obtain the results for our simulation example where $\sigma = 0.3$:

$$\begin{cases} \kappa_{var}^{B\&S} = 0.0900, \\ \kappa_{var}^{AY} = 0.0807 < \kappa_{var}^{B\&S}, \\ \kappa_{var}^{RevAY} = 0.1064 > \kappa_{var}^{B\&S}. \end{cases}$$

The difference between κ_{var}^{AY} and κ_{var}^{RevAY} may come from the opposite directions of jumps. In fact,

$$(\ln(1-x))^2 - (\ln(1+x))^2 = 2x^3 + O(x^5).$$

If we conjecture that the Azéma-Yor fake GBM paths and the reversed Azéma-Yor fake GBM paths have similar jumping occurrences and the sizes of the jumps are of similar scale, then the reversed AY fake GBM, which always has down-sided jumps, is the one with greater quadratic variation for the logarithm.

For the variance swap, we see that the quadratic variation of the logarithm of the fake GBM can be either bigger or smaller than that of the classical geometric Brownian motion.

Chapter 5

Conclusion and Final Remarks

In this thesis, we are interested in the notion of fake geometric Brownian motions. We construct two fake geometric Brownian motion processes via the solutions to the Skorokhod embedding problem. One process, which we call Azéma-Yor fake GBM, is continuously decreasing except some up-sided jumps. The other one, the reversed Azéma-Yor fake GBM, is continuously increasing except some down-sided jumps. The latter one represents some property in real with a long-term perspective. However, neither of the two reflects the real stock prices very well due to the local regularity of the paths. It is interesting to see that processes with such different behaviours have the same marginal densities, and reproduce the same flat IV surface.

Furthermore, we price options with underlying stock following these two fake processes. By pricing the European call option, we verify that the numerical result is consistent with the theoretical one, and thus confirm that our numerical implementation works for further option pricing study. By pricing three exotic path-dependent options: the one-touch option, the fixed-strike Asian option, and the variance swap, we see that the distribution of the maximum on path, the distribution of the path average, and the quadratic variation of the logarithm are all distinct for the two fake GBM processes from the classical geometric Brownian motion.

We note that our constructed fake geometric Brownian motion processes are not continuous, and we remark that there is no direct way to construct a continuous fake GBM using the exponential of a fake Brownian motion. Thus, the question whether there exists such a continuous fake geometric Brownian motion is left open.

Appendix A

Code Resources

In this thesis, for the programming aspect, most parts of the code are written originally except for the Brownian bridge paths. The essential parts of generating the stock price at maturity and the stock price path for the constructed processes are presented in Chapter 3 under the form of pseudo-code. The other codes are mostly basic programmes for option pricings and Monte Carlo simulation, and we do not provide them here due to the large number of programmes. For generating Brownian bridge paths, we have referred to the pseudo-code in the book *Monte Carlo Methods in Financial Engineering* ([5], 3.1).

Bibliography

[1] J.M.P. Albin. A continuous non-brownian motion martingale with brownian motion marginal distributions. *Statistics and Probability Letters*, **Volume 78, Issue 6**:682–686, 2008.

[2] J. Azéma and M. Yor. Une solution simple au problème de skorohod. *Séminaire de Probabilités XIII, Lecture Notes in Mathematics*, **Volume 721/1979**:90–115, 1979.

[3] L. Bachelier. Théorie de la spéculation. *Annales Scientifiques de L'Ecole Normale Supérieure*, **17**:21–88, 1900.

[4] S. Black and M. Scholes. The pricing of options and corporate liabilities. *The Journal of Political Economy*, **Vol. 81, No. 3**:637–654, 1973.

[5] P. Glasserman. *Monte Carlo Methods in Financial Engineering*. Springer, 2003.

[6] K. Hamza and F.C. Klebaner. A family of non-gaussian martingales with gaussian marginals. *Journal of Applied Mathematics and Stochastic Analysis*, **Volume 2007**:Article ID 92723, 19 pages, 2007.

[7] J.-F. Le Gall. Notes de cours de master 2: Calcul stochastique et processus de markov. *Master Probabilités et Statistiques, Université Paris-Sud*, 2010.

[8] D.B. Madan and M. Yor. Making markov martingales meet marginals: With explicit constructions. *Bernoulli*, **8(4)**:509–536, 2002.

[9] J. Obłój. The skorokhod embedding problem and its offspring. *Probability Surveys*, **Volume 1**:321–392, 2004.

[10] J. Obłój. Financial derivatives ii: Problem sheet 1 & correction. *Mathematical Institute, University of Oxford*, 2011.

[11] K. Oleszkiewicz. On fake brownian motions. *Statistics and Probability Letters*, **Volume 78**:1251–1254, 2008.

[12] Z. Qian. Lecture notes: Stochastic differential equations. *Mathematical Institute, University of Oxford*, 2008.

[13] P.A. Samuelson. Proof that properly anticipated prices fluctuate randomly. *Industrial Management Review*, **6:2**:41–49, 1965.

[14] S.E. Shreve. *Stochastic Calculus for Finance II: Continuous-Time Models*. Springer, 2004.

[15] A.V. Skorokhod. *Studies in The Theory of Random Processes*. Translated from the Russian by Scripta Technica, Inc. Addison-Wesley Publishing Co., Inc., Reading, Mass., 1965.